structure of warwickite is slightly different from those of pinakiolite and ludwigite. Let us picture to ourselves a hypothetical arrangement of oxygen atoms which consists of only four piled layers (two hexagonal and two quadratic), instead of five as in pinakiolite. If now we outline in this arrangement the unit cell of warwickite in the position shown in Fig. 6 (*d*) and then let it slip alternately upwards and downwards by an amount $\frac{1}{2}b$ parallel to (100), making an angle of about 64° with the plane of layers (Fig. 6 (*c*)), we shall obtain the very arrangement of oxygen atoms characteristic of the structure of warwickite (see Fig. 1). It is interesting to note that the cleavage of pinakiolite occurs parallel to the layers, i.e. (001), while that of warwickite is parallel to the plane of slips, i.e. (100).

These relationships between various arrangements of oxygen atoms underlying the structures of warwickite, ludwigite and pinakiolite are all the more interesting, since we have previously found similar phenomena in the wollastonite group (Ito, 1949, p. 110). One of the present writers in collaboration with R. Sadanaga and Y. Takéuchi, basing his argument on the experimental evidences obtained by him as well as by Barnick, has demonstrated that we can derive the structure of monoclinic as well as triclinic wollastonite from another monoclinic wollastonite, protowollastonite, by slipping its cells alternately or stepwise. Although analogy here is only partial and the mechanism applies in this case only to the arrangements of oxygen atoms, and not to the entire structures as in wollastonite, it is nevertheless very interesting in view of the dominant role of oxygen in the genesis of minerals (see, for example, Barth (1948)).

References

Barth, T. F. W. (1948). *J. Geol.* **56**, 50.

Bradley, W. M. (1909). *Amer. J. Sci.* **27**, 179.

Bragg, W. L. (1937). *The Atomic Structure of Minerals.* Ithaca: Cornell University Press.

Des Cloizeaux, A. L. O. L. (1874). *Manuel de Minéralogie*, **2**. Paris: Dunod.

Flink, G. (1891). *Z. Krystallogr.* **18**, 361.

Geijer, P. (1924). *Econ. Geol.* **19**, 687.

Ito, T. (1949). *X-ray Studies on Polymorphism.* Tokyo: Maruzen.

Mallard, E. (1888). *Bull. Soc. franç. Miner.* **2**, 165.

Palache, C. (1929). *Amer. Min.* **14**, 43.

Shannon, E. V. (1921). *Proc. U.S. Nat. Mus.* **59**, 667.

Taylor, W. H. & West, J. (1928). *Proc. Roy. Soc.* A, **117**, 517.

Watanabé, T. (1939). *Miner. petrogr. Mitt.* **50**, 441.

Acta Cryst. (1950). **3**, 107

The Interpretation of Diffuse X-ray Diagrams of Carbon

By Rosalind E. Franklin

Laboratoire Central des Services Chimiques de l'État, 12 quai Henri IV, Paris IV, France

(*Received* 4 *June* 1949 *and in revised form* 2 *July* 1949)

Measurements on a carbon prepared by pyrolysis of polyvinylidene chloride at 1000° C. have been used to study methods of interpretation of the diffuse X-ray diagrams given by non-graphitic carbons. Results obtained from a Fourier integral analysis are in satisfactory agreement with those deduced from a comparison of the experimental intensity curve with an intensity curve calculated for a hypothetical structure. For the high-angle part of the diagram the latter method is found to be preferable; it is less tedious, and gives the results with greater precision. The Fourier transform of the low-angle scattering is, however, of value.

It is concluded that, in the carbon investigated, 65 % is in the form of highly perfect and planar graphite-like layers of mean diameter 16 A., and 35 % is in a much less organized state, giving only a gas-like contribution to the X-ray scattering. About 55 % of the graphite-like layers are grouped in pairs of parallel layers with an interlayer spacing of 3·7 A., and the remaining 45 % show no mutual orientation. There is a mean interparticle distance of about 26 A.

Introduction

The general form of the X-ray diagrams given by non-graphitic carbons is well known. Diffuse bands are observed corresponding approximately to the positions of the (002), (100) and (110) reflexions of graphite, and there is often strong low-angle scattering. The degree of sharpening of the bands is frequently considered as a measure of progress towards graphite. The general trend of the phenomenon has been extensively investigated by Riley and his collaborators (Blayden, Gibson & Riley, 1944) who have studied the influence of temperature on many different carbons. Warren (1934), in a quantitative study of a carbon black, confirmed by Fourier integral analysis the existence of interatomic distances close to those within a single graphite layer. A further important advance was made by Warren

(1941) when he developed a quantitative theory of random-layer lattices and showed that non-graphitic carbons gave diffraction bands of the form given by such lattices (Biscoe & Warren, 1942).

Following Warren's study of a single carbon black, a large amount of quantitative work on carbons of different origin subjected to different treatments is required for the solution of the many outstanding problems in carbon structure. Examples of such problems are the causes of the differences in structure and properties shown by carbons prepared under the same conditions from different starting materials; the relationship between structure, as revealed by X-rays, and colloidal properties as studied by adsorption and surface-area measurements; and the nature and kinetics of the crystallization process which ultimately leads to the formation of graphite.

In the past the emphasis has been on the resemblance between carbon and graphite. It is supposed by Riley, Warren and others that carbons contain minute crystallites (composed of graphite-like layers stacked parallel to one another but not otherwise mutually orientated) in a matrix of carbon in a less highly ordered state. Estimates have been made of the dimensions of the crystallites, but not of the proportion of the total carbon which they represent. It is obvious, however, that the nature and extent of the non-organized part and the mutual disposition of the crystallites must be of supreme importance in determining the course of any subsequent structural changes induced by thermal or other treatment.

As a preliminary to the wider problems indicated above, it seemed desirable to make a detailed study of one non-graphitic carbon to find just how much information the diffuse X-ray diagram could be made to yield. This preliminary study forms the subject of the present paper. Quantitative measurements have been made of the complete X-ray diagram, including the low-angle scattering. Different methods of interpretation have been applied and the relative merits of the different methods are discussed. The inclusion of measurements at very small and very large angles of scattering, and the study not only of the shape but also of the absolute intensities of the diffuse bands, have led to a more detailed picture of the structure than has hitherto been obtained for any one carbon.

Material

Since the object of the investigation was to study the ways in which the structure of various carbons may differ from that of graphite, it was desirable to work with a highly disordered carbon. At the same time, to facilitate quantitative work, the carbon should be as pure as possible. A pure carbon may be produced from any organic material by heating to a sufficiently high temperature, but the higher the temperature the more nearly the structure approaches that of graphite. The problem was therefore to prepare a pure carbon at a relatively low temperature.

It is well known that organic materials containing hydrogen and chlorine lose HCl on heating. The polymer $(C_2H_2Cl_2)_n$ was therefore sought, in the hope that it would readily lose HCl and leave pure carbon. In practice the material 'Saran', a copolymer of $C_2H_2Cl_2$ with a small quantity of C_2H_3Cl, was used. Prolonged heating at 600° C. sufficed to remove all the chlorine. The sample selected for detailed study was prepared by heating for 2 hr. at 1000° C. in oxygen-free nitrogen. Analysis gave 99·4–99·6 % C.

The material was obtained in the form of a highly swollen coke showing a metallic lustre. This was subsequently ground to form a hard black powder. It has a high adsorption capacity, and the surface area measured by low-temperature nitrogen adsorption is 1300 $m.^2g.^{-1}$, an exceptionally large value. (I am indebted to Monsieur J. Escard for this measurement.)

Experimental

Cu $K\alpha$ and Mo $K\alpha$ monochromatic radiation, obtained with a bent-quartz focusing monochromator, were used with a cylindrical vacuum camera of diameter 76 mm.

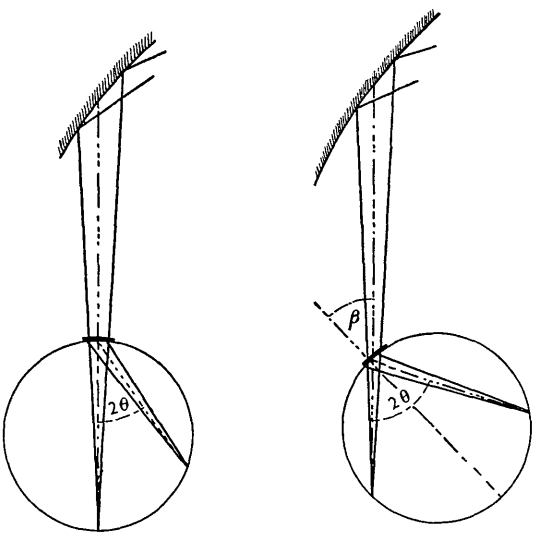

Fig. 1. (*a*) Symmetrical position of camera. (*b*) Unsymmetrical position.

Photographs were taken by transmission, the symmetrical position (Fig. 1 (*a*)) being used for diffraction angles up to 27° and the unsymmetrical arrangement (Fig. 1 (*b*)) for angles up to 50° (Guinier, 1939). The sample was in the form of a platelet of thickness 0·6 mm. formed by agglomerating the powdered material with 1·5 % by weight of glue. For calibration of the camera diameter, a similar sample containing a small quantity of fine aluminium powder was used.

The films were microphotometered with a Leeds-Northrup automatic recording instrument, and on each

film only that part having a photographic density between 0·1 and 0·7 was used. The zero of photographic density was obtained by placing a band of lead against the film near the equator during each exposure.

The intensity curves obtained when the focusing camera is used require to be corrected for the variation with the angle of diffraction of the distance between sample and film, and also for the variation of the angle of incidence on the film of the diffracted X-rays. The former correction is of the form $\cos 2\theta$. The latter was obtained experimentally in the form of a continuous photographic trace giving directly the dependence of photographic density on the angle of incidence. The calibration was carried out for Cu and Mo radiation.

To obtain the absorption correction, the absorption in the sample for transmission at perpendicular incidence was measured by photographing a uniform monochromatic beam in which the sample was allowed to form a shadow. The low-angle part of the intensity curve was corrected for the influence of the finite height of the X-ray beam by a method described elsewhere (Franklin, 1950).

Finally, before fitting the different intensity curves obtained with Cu and Mo radiation, it is necessary to apply the correction for the state of polarization of the incident and diffracted radiation which is given by

$$(1+\cos^2 2\alpha \cos 2\theta)/(1+\cos^2 2\alpha),$$

where α is the angle of reflexion in the monochromator.

After applying the above corrections, some twenty-five diagrams, obtained with Cu and Mo radiation, with different times of exposure and with different angles of incidence, were used to construct the total scattering curve for values of $2\sin\theta/\lambda$ from 0·01 to 2·20.

It may be mentioned here that the advantages of the focusing camera are good resolution and reasonably short exposures with a small sample. The disadvantages are the limited angular range obtained on any one photograph, and the rather numerous corrections which have to be applied to the experimental intensity curve.

X-ray data

The corrected intensity curve is given in Fig. 2, curve I, where the positions of the (002) and (*hk*0) graphite lines are also indicated. It is seen that the (002) band is extremely weak and diffuse, and merges with the very extensive low-angle scattering. In the neighbourhood of the (100) and (110) graphite lines there are two-dimensional (10) and (11) bands such as are observed for most carbons. In addition, careful measurements at larger angles reveal a further series of maxima all of which may be related to (*hk*0) reflexions of graphite. Higher orders of the (002) band are not observed, nor are there any (*hkl*) ($l \neq 0$) reflexions.

From mere inspection of the diagram it may therefore be inferred that the carbon contains graphite-like layers which are well-ordered in two dimensions but show little tendency to parallel stacking and no three-dimensional crystalline order. Two methods have been used to investigate the structure in more detail. First, a Fourier integral analysis of the intensity curve was used to obtain the mean spherical atomic distribution. Secondly, Warren's theory of the diffraction by a two-dimensional lattice was used to calculate a complete intensity curve which was compared with the experimental curve.

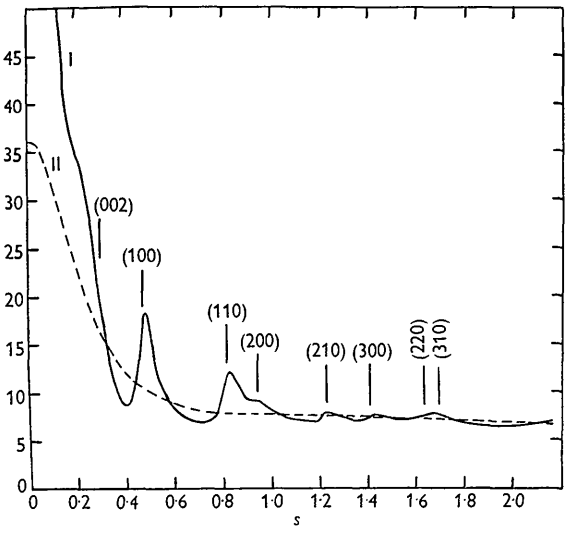

Fig. 2. Curve I, corrected intensity curve. Curve II, independent scattering curve.

Fourier integral analysis

The mean atomic distribution about any given atom was obtained by the method of Debye & Menke (1931), which has been applied extensively to liquids and amorphous materials (e.g. Warren, 1934; Gingrich, 1943). For a substance containing only one kind of atom and having a continuous atomic density function $\rho(r)$ such that $4\pi r^2\rho(r)\,dr$ is the mean number of atoms whose distance from any given atom lies between r and $r+dr$, the intensity of coherent scattering is given by the equation

$$si(s) = 2\int_0^\infty r\rho(r)\sin(2\pi sr)\,dr,$$

where

$$s = 2\sin\theta/\lambda,$$

$$i(s) = I/Nf^2 - 1,$$

I is the intensity of coherent scattering, in electron units, after correction for absorption, polarization and geometrical factors, N is the number of scattering atoms in the path of the X-ray beam, and f is the atomic scattering factor.

Applying the Fourier inversion,

$$r\rho(r) = 2\int_0^\infty si(s)\sin(2\pi sr)\,ds,$$

or

$$4\pi r^2\rho(r) = 8\pi r\int_0^\infty si(s)\sin(2\pi sr)\,ds. \qquad (1)$$

Limits of numerical integration

In the case of a single homogeneous scattering substance of normal dimensions the integral in equation (1) consists of two distinct parts, due respectively to the observable intensity function $i(s)$ and to the unobservable peak function which occurs in the neighbourhood of $s=0$. The content of the latter is independent of the structure and would have the same value for a similar volume of continuous scattering substance of uniform density equal to ρ_0, the macroscopic density of the material considered. For such a continuous, uniform substance $i(s)$ would be zero for all values of s greater than a very small value which is experimentally inaccessible (the exact value depends on the size and shape of the scattering material). The experimentally observed values of $i(s)$ are due to the deviations of ρ from ρ_0 in the real substance. We may therefore write

$$4\pi r^2\{\rho(r)-\rho_0\}=4\pi r^2\Delta\rho=8\pi r\int_0^\infty si(s)\sin(2\pi sr)\,ds, \quad (2)$$

where here the integral, although extending to $s=0$, contains only the observable intensity function.

In finely divided solids which show low-angle scattering, part of the zero-angle intensity peak becomes spread over measurable values of s. In many cases the low-angle scattering is nevertheless sharply separated from the rest of the diffraction pattern. The integration in equation (2) may then be carried out for the function $si(s)$ excluding the low-angle scattering. In the present case, however, the extensive low-angle scattering is inseparable from the rest of the diffraction pattern, and must therefore be included in the integral. Measurements were made to values of s as small as the experimental arrangement permitted ($<0{\cdot}1$), and the intensity extrapolated to $s=0$. There remains, however, a modified unobservable peak function at $s=0$. The contribution of this in equation (2) is $4\pi r^2\rho_0$, where ρ_0 is no longer the true density of the diffracting substance, but the mean density of the particles together with such spaces between them as are responsible for the accessible low-angle scattering. If, for example, the dispersion of the fine particles were increased, the observable low-angle scattering would increase at the expense of the unobservable peak function, and the value of ρ_0 would further decrease.

Owing to the somewhat arbitrary value of ρ_0, which cannot readily be measured with any certainty, only $\Delta\rho$ and the function $4\pi r^2\Delta\rho$ will be considered in what follows.

The upper limit of the integral in equation (2) is $s=\infty$. In practice it is necessary to impose a finite upper limit to the integration at $s=S$ and to assume that $i(s)$ is zero for all values of s greater than S. This is further discussed below.

Calculation of $si(s)$

To calculate the function $si(s)$ the corrected experimental intensity curve (Fig. 2, curve I) was obtained in electron units, and the incoherent scattering was subtracted by making use of the intensity values at large angles of scattering. The principle of this method, as normally applied, is that for non-crystalline materials the interference effects at large angles are negligible and the observed intensity is equal to the independent scattering (coherent + incoherent), i.e. $f^2+I_{\text{inc.}}$, where $I_{\text{inc.}}$ is the incoherent scattering. In the present case, interference effects at large angles are not negligible, but, since measurements were made for values of s up to 2·2, at which point the coherent scattering is only 12 % of the total independent scattering, there is little scope for error in placing the independent scattering curve (Fig. 2, curve II).

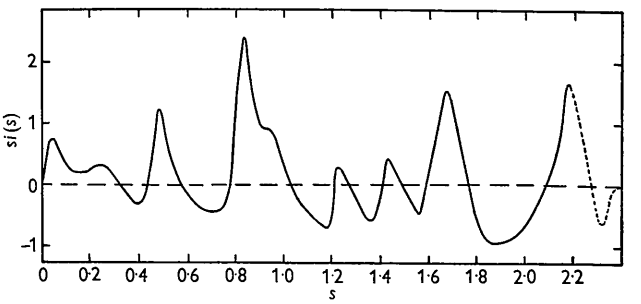

Fig. 3. The function $si(s)$.

The form of the independent scattering curve shown in Fig. 2 is derived from the values of $I_{\text{inc.}}$ tabulated by Compton & Allison (1935) and the atomic scattering factor calculated by James & Brindley (1931). The function $si(s)$ obtained from the experimental intensity curve after subtraction of the incoherent scattering and division by f^2 is shown in Fig. 3. It is clear that a maximum in $si(s)$ occurs near $s=2{\cdot}2$. This last peak was therefore assumed to have approximately the same shape as the preceding ones, and $si(s)$ was assumed to come to zero at $s=2{\cdot}4$ in the manner indicated in the figure.

The atomic distribution function

For calculation of $4\pi r^2\Delta\rho$ (equation (2)) it was assumed that $si(s)=0$ for $s>2{\cdot}4$, and the integral was replaced by the sum of 120 terms $si(s)\sin(2\pi sr)\,\Delta s$ spaced at intervals of $0{\cdot}02(=\Delta s)$ in s. This approximation leads to a function $r\Delta\rho$ which is periodic, the full period being $1/\Delta s=50$ A. It may therefore be used to obtain $4\pi r^2\Delta\rho$ for values of r up to $1/2\Delta s=25$ A. only if $\Delta\rho$ is zero for all values of r greater than 25 A. In reality this condition is not exactly fulfilled, and the accuracy of the calculation is therefore somewhat reduced for the larger values of r.

In Fig. 4 the function $4\pi r^2\Delta\rho$ calculated in this way is shown for values of r up to 9 A. Ordinates were calculated for values of r at intervals of 0·21 A., intermediate points being obtained where necessary in the neighbourhood of important maxima or minima. The interatomic distances within a single graphite layer are also indicated at the base of the figure, the height of the

lines being proportional to the number of neighbours at a given distance. It is clear that maxima exist in the density function at distances corresponding approximately to the interatomic distances in a graphite layer. But there are certain features of the curve which are obviously false. There are maxima and positive values of $\Delta\rho$ at 0·4 and 0·8 A., whereas in reality, for distances less than the smallest interatomic distance, ρ must be zero, and $4\pi r^2\Delta\rho$ must therefore be equal to $-4\pi r^2\rho_0$. Further, for any reasonable value of ρ_0 which may be assumed, the minima at 1·7 and 2·1 A. would lie below the curve $-4\pi r^2\rho_0$, and consequently represent negative density values. The strong maximum at 1·9 A. does not represent any known carbon–carbon distance. These and other less striking anomalies in Fig. 4 may result from either of two effects which will be considered separately.

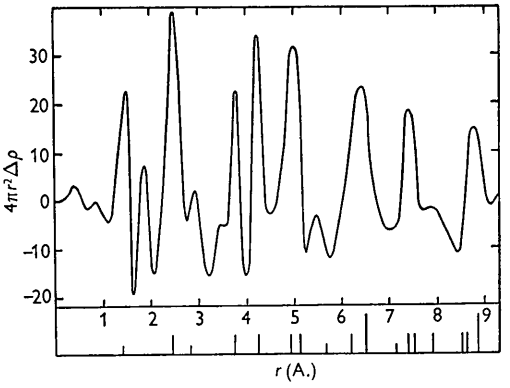

Fig. 4. Above, the atomic distribution function obtained by direct use of the corrected intensity curve. Below, interatomic distance in a graphite layer-plane.

The assumption that $si(s)=0$ for $s>2{\cdot}4$ is not justified, as is evident from inspection of Fig. 3. Measurements of $i(s)$ for larger values of s cannot, however, be made with any reasonable accuracy by the photographic method owing to the preponderance of incoherent scattering. Abrupt termination of the curve at $s=2{\cdot}4$ may be expected to lead to secondary interference effects in the transform function $r\Delta\rho$. This problem has been discussed by Bragg & West (1930) and by James (1948) for the case of crystals. Direct use of the experimental curve limited to values of s between 0 and S is equivalent to multiplying the true function $si(s)$ by a function $\phi(s)$ which takes the value unity for $s<S$ and zero for $s>S$. This has the effect of 'folding' the transform of $\phi(s)$ into the true transform function $r\Delta\rho$ (Ewald, 1940). In a one-dimensional analysis, the transform of $\phi(s)$ is given by $2S\frac{\sin 2\pi Sr}{2\pi Sr}$, which has maxima at $r=0$, $\pm\frac{5}{4S}$, $\pm\frac{9}{4S}$, etc., and minima at $r=\pm\frac{3}{4S}$, $\pm\frac{7}{4S}$, etc. It follows that for $S=2{\cdot}4$ each peak in $r\Delta\rho$ (or in $4\pi r^2\Delta\rho$) will have on either side of it a secondary maximum at a distance of 0·52 A. and minima at a distance of 0·31 and 0·73 A. It is thus abundantly clear from Fig. 4 that the secondary peaks associated with the maxima at 1·4 and 2·4 A. combine to give the strong spurious peak at 1·9 A., and the diffraction minima combine to give the exaggerated minima at 1·7 and 2·1 A.

To avoid these secondary interference effects it is customary to multiply the observed intensity function by $\exp[-b^2s^2]$, where b is an arbitrary constant. Although this has been referred to as an 'artificial temperature factor' it is in no way related to a real temperature correction. The optical equivalent is the substitution of a simple aperture by a graduated diaphragm. The Gaussian form is selected because it is the most effective in suppressing secondary interference while reducing as little as possible the resolving power (which is determined originally by the limiting value S of s). Numerical calculation shows a suitable value of b to be one which gives $\exp[-b^2s^2]$ equal to about 0·1 for $s=S$. Hence in the present case the function $\exp[-0{\cdot}4s^2]$ was used.

In the transform of $si(s)\exp[-0{\cdot}4s^2]$ the maximum at 1·9 A. was entirely suppressed, and the depth of the minimum in this region greatly reduced. The maxima at 0·4 and 0·8 A., however, persisted. These maxima can only be due to the use of an incorrect atomic scattering factor.

The complete function $\Delta\rho$ contains an infinitely narrow peak at $r=0$. This peak is the transform of the independent coherent scattering curve which, in the present analysis, has been subtracted from the total coherent scattering to give $i(s)=I/Nf^2-1$. If values of f, and hence of the independent scattering, are incorrect, the subtraction of the peak in $\Delta\rho$ at $r=0$ will be inexact, and distortion of the function $\Delta\rho$ in the neighbourhood of $r=0$ will result. Inspection of the numerical calculation of the integral showed that the maxima at 0·4 and 0·8 A. could be reduced by using a larger atomic scattering factor in the low-angle region, especially for values of s between 0·4 and 0·6. The scattering factor was therefore modified somewhat arbitrarily as shown in Fig. 5 and the calculation repeated. The function $4\pi r^2\Delta\rho$ obtained in this way is shown in Fig. 6, curve I.

Fig. 6, curve II, shows the function $4\pi r^2\Delta\rho$ which would be given by a single infinite graphite layer under the same conditions. That is, the curve represents the fluctuations which would be observed in the function $4\pi r^2\rho$ due to the atomic distribution within individual graphite layers in any carbon which consisted entirely of such layers, of perfect structure and of diameter large compared with the values of r considered. To obtain this curve account was taken of the function $\exp[-b^2s^2]$ introduced above, which has the effect of replacing each infinitely narrow peak of content A in the true function $r\Delta\rho$ by a function of the form

$$A\frac{\sqrt{\pi}}{b}\exp\left[-\frac{\pi}{b^2}r^2\right].$$

In Fig. 6 there is sufficient resemblance between curves I and II to prove conclusively that the carbon contains graphite-like layers. The amplitude of the fluctuations in curve I is, however, consistently less than in curve II, the difference increasing with increasing values of r. Here three factors must be distinguished:

(1) The structure of the graphite-like layers may be imperfect. This would render the peaks weaker and more diffuse, the magnitude of the effect increasing rapidly with increasing r.

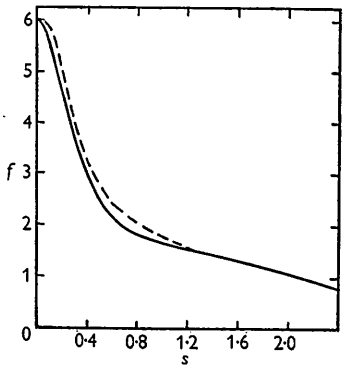

Fig. 5. The atomic scattering factor. Full line, due to James & Brindley; broken line, as modified to reduce the peaks at 0·4 and 0·8 A. in Fig. 4.

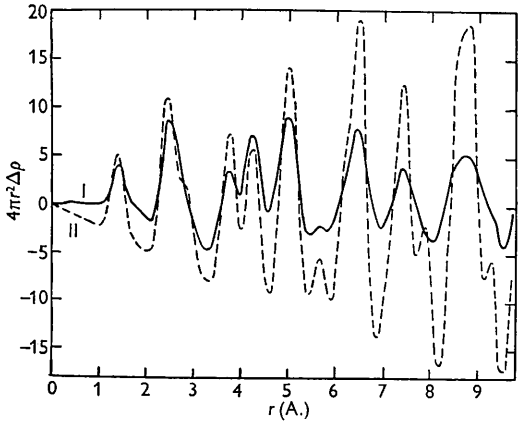

Fig. 6. Curve I, the atomic distribution function obtained after multiplying the corrected intensity curve by $\exp(-0{\cdot}4s^2)$. Curve II, the function which would be given by a single infinite graphite layer under the same conditions.

(2) It is possible that not all of the carbon is in the form of graphite-like layers. This would reduce the amplitude for the whole curve, independently of the value of r.

(3) The graphite-like layers may be perfect but very small. The form of the peaks would be unchanged, but the amplitude would decrease with increasing r.

From Fig. 6 it is clear that the influence of (1) is extremely slight, the shape of the peaks in the two curves being closely similar. In particular, the apparition of the small peak at 5·6 A. and the form of the well-isolated peak at 6·4 A. show that even for relatively large values of r the influence of structural imperfections is negligible. The difference between the amplitudes of the experimental and theoretical peaks at small distances (1·4 and 2·45 A.) can therefore certainly not be attributed to disorder. It must be assumed that (2) is operative. The ratio of the observed and calculated amplitudes for small values of r is about $\frac{2}{3}$, indicating that about $\frac{2}{3}$ of the carbon is in the form of graphite-like layers. The remaining $\frac{1}{3}$ makes no measurable contribution to the function $4\pi r^2\Delta\rho$, and must be in a much less highly organized state.

To account for the decreasing amplitude with increasing r in curve I as compared with curve II (Fig. 6) it must be supposed that the layers, though perfect, are sufficiently small for the number of atoms at distance r from a given atom to be significantly reduced for values of r greater than a few Ångström units. From the magnitude of this effect a rough estimate of the diameter of the layers can be made.

For a circular layer of diameter L the number of atoms at distance $r=aL$ from a given atom is given by n_aP_r, where P_r is the number for an infinite layer, and n_a is the area in common between two circles of unit area (diameter $2/\sqrt{\pi}$) whose centres are at a distance $2a/\sqrt{\pi}$ apart (cf. Wilson (1948, p. 37)). The dependence of n_a on a is such that for $n_a=0{\cdot}5$, $a=0{\cdot}4$. In Fig. 6 the ratio of observed to theoretical amplitudes decreases from about $\frac{2}{3}$ for small values of r to about $\frac{1}{3}$ at $r=7$ A., thus indicating a layer diameter of between 15 and 20 A.

The possible influence of mutual orientation of the graphite-like layers has not so far been considered. It is clear that the general rise in curve I (Fig. 6) in the neighbourhood of 3·7–4·4 A. must be attributed to a weak diffuse maximum at about 4 A. due to the interlayer spacing.

The particle distribution function

The function $4\pi r^2\Delta\rho$ was given in Fig. 6 for values of r up to 9 A. only. The limitation is due to the method of numerical calculation, which gives results decreasing in accuracy with increasing r and becoming valueless as r approaches 25 A. The method is also extremely tedious.

Since the graphite-like layers are only 15–20 A. in diameter, it may be expected that, for values of r larger than this, fluctuations in density due to the structure of a single graphite layer will not be observed. Any fluctuations observed at large distances must represent the form and spatial distribution of the layers or groups of layers. That is, for large values of r the density function is essentially the Fourier transform of the low-angle scattering. To obtain $4\pi r^2\Delta\rho$ for values of r approaching 50 A. the calculation was therefore simplified by using only the low-angle part of the experimental scattering curve. The accuracy was increased by the use of an improved method of numerical calculation devised by V. Luzzati (private communication). Among other advantages, the method gives directly values of $r^3\Delta\rho$ (the normal method gives $r\Delta\rho$) and is therefore of

value for obtaining with reasonable accuracy the weak and diffuse density fluctuations which occur at large values of r.

The transform of the low-angle scattering alone (taking $si(s)=0$ in the region of s where in reality the (002) and (hk) bands are observed) would represent a structure consisting of fine particles which have the same form and spatial distribution as those in the real structure but which are continuous and uniform in density. In the present case separation of the low-angle scattering from the very weak and diffuse (002) reflexion would be arbitrary and meaningless. The transform was therefore calculated for the low-angle scattering taken together with the (002) reflexion but excluding the (hk) bands. It therefore represents a structure in which the graphite-like layers are replaced by continuous and uniform layers of the same mean surface density; it may therefore be expected to give some information about the spatial distribution of these layers.

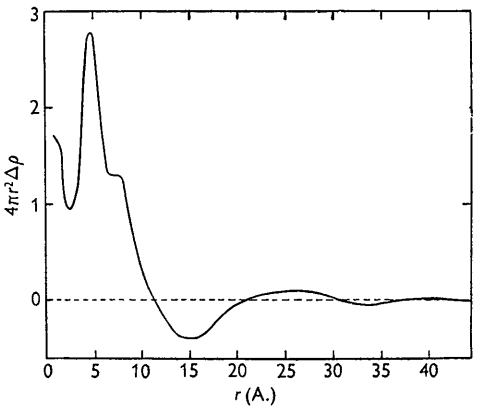

Fig. 7. The particle distribution function obtained from the Fourier transform of the low-angle part of the corrected intensity curve.

For the numerical calculation, the experimental values of $i(s)$ were used for values of s up to 0·32, and, for $s>0{\cdot}32$, $i(s)$ was assumed to approach the curve calculated for diffraction by isolated graphite-like layers (see below), joining this curve at $s=0{\cdot}40$. The function $4\pi r^2\Delta\rho$ obtained in this way is shown in Fig. 7. There is, as would be expected, a peak corresponding to the spacing between parallel layers. The maximum occurs at about 4·5 A. in $4\pi r^2\Delta\rho$ and 4·2 A. in $\Delta\rho$. The preceding minimum occurs at about 2·5 A. in $4\pi r^2\Delta\rho$ and 3·3 A. in $\Delta\rho$. In the ideal function ρ for a structure containing parallel layers of no thickness the curve rises perpendicularly from a minimum to a maximum at a value of r equal to the interlayer spacing. Blurring of the experimental curve due to the limitations of measurement and of calculation results in the interlayer spacing lying about halfway between the maximum and the preceding minimum. Thus the interlayer spacing is about 3·5–3·8 A.

In addition to the peak at 4·5 A. the function $4\pi r^2\Delta\rho$ shows a diffuse minimum at 15 A. and a weak but perfectly definite diffuse maximum between 24 and 28 A. It is clear that the position of the minimum is closely related to the diameter of the graphite-like layers. The diffuse maximum must represent the mean distance between neighbouring particles. The exact nature and shape of these particles cannot be determined from this curve alone, but, taking into account that only about $\frac{2}{3}$ of the total carbon is involved in the graphite-like layers of diameter 15–20 A. and that the remaining $\frac{1}{3}$ of less highly organized structure is presumably distributed around the edges of these layers, it seems that each particle must contain only a very small number of layers, possibly only one parallel-layer group.

To summarize, Fourier analysis has shown that about two-thirds of the carbon is in the form of highly perfect graphite-like layers of diameter 15–20 A. arranged in small groups of parallel layers with an inter-layer spacing of 3·5–3·8 A. The remaining one-third of the carbon is in a highly disordered state. The graphite-like layers are contained in small groups or particles having a mean separation of about 26 A.

It will now be shown that, with the exception of the inter-particle spacing of 26 A., the same information can be obtained with rather more precision and less labour by an alternative method.

Calculation of the intensity curve

It has been shown above that inspection of the X-ray diagram indicates that the carbon contains graphite-like layers but no three-dimensional crystalline order. Only (00l) and two-dimensional (hk) bands are observed.

Warren (1941), in a theoretical study of diffraction by random-layer lattices, has developed equations giving both the form and absolute intensity of the (hk) bands in terms of the layer dimension, L, and the position, s_0, of the related ($hk0$) crystalline reflexion. He has also shown (Biscoe & Warren, 1942) that the form of the (10) band in the carbon black investigated by him agreed well with his equations, but the comparison was made for one band only, and absolute intensities were not discussed. Warren's theory will now be applied to the analysis of the (hk) bands given by the present carbon.

The intense part of the band is given by

$$I=K\frac{mF^2}{2\sqrt{2}\,\pi nA_a}\left(\frac{L}{\sqrt{\pi}}\right)^{\frac{1}{2}}s^{-\frac{3}{2}}F(a), \qquad (3)$$

where K is the intensity of independent scattering by the same material, m is the two-dimensional multiplicity, F is the structure factor of the unit cell in a single layer, A_a is the area of the unit cell, n is the number of atoms per unit cell, and $F(a)=\int_0^\infty \exp[-(x^2-a)^2]\,dx$,

where $$a=\sqrt{\pi}\,L(s-s_0). \qquad (4)$$

Numerical values of $F(a)$ are tabulated by Warren (1941).

The intensity of the high-angle part of the band, remote from the position of the related ($hk0$) reflexion, is independent of L and is given by

$$I = K\frac{mF^2}{4\pi n A_a} s^{-1}(s^2 - s_0^2)^{-\frac{1}{2}}. \qquad (5)$$

The formula given by Warren for the determination of L, the layer dimension, is

$$L = \frac{3{\cdot}26}{\sqrt{\pi\,\delta s}},$$

where δs is the half-peak width of the band. This formula, derived from equation (4), leads to values of L which are too large in the case of very small layers (i.e. very diffuse bands) since it takes no account of the variation within the band of $s^{-\frac{3}{2}}$ in equation (3). A better value of L is obtained from the half-peak width as follows.

Let s_1 and s_2 be the positions of half-maximum intensity on the low- and high-angle sides of the band respectively, $s_{\max.}$ the position of maximum intensity, and $F(a)_{\max.}$ the maximum value of $F(a)$. Then, from equation (3),

$$F(a_1) = \tfrac{1}{2}F(a)_{\max.}(s_1/s_{\max.})^{\frac{3}{2}} \quad \text{at } s_1$$

and

$$F(a_2) = \tfrac{1}{2}F(a)_{\max.}(s_2/s_{\max.})^{\frac{3}{2}} \quad \text{at } s_2.$$

From the numerical values of $F(a)$ and a given by Warren, a_1 and a_2 are determined, and, from equation (4), the layer dimension is given by

$$L = \frac{a_2 - a_1}{\sqrt{\pi\,(s_2 - s_1)}} = \frac{a_2 - a_1}{\sqrt{\pi\,\delta s}}.$$

Even this method tends to lead to values of L which are slightly high, since it depends on accurate measurement of the position of maximum intensity. The procedure adopted was therefore to use this method to determine L approximately, and then, by fitting the experimental curve with curves calculated for the whole band, to obtain L with greater precision by trial-and-error. In this way it was established that the best value of L for the present carbon is 16 ± 1 A.

Having determined the layer dimension, the experimental intensities, which are available in absolute units, may now be compared with those given by equations (3) and (5), with a view to determining what proportion of the carbon is involved in the layer structure. For this purpose the layer is assumed to be identical with the graphite layer, giving $A_a = 5{\cdot}25$ A.^{2} and $n = 2$. In equations (3) and (5) it is then found that the intensity of the (10) band is greater than the theoretical intensity. The intensity of the (11) band, on the other hand, is only 65 % of the theoretical intensity. Higher-order bands are weaker and measurable with much less accuracy (owing to the low atomic scattering factor and strong incoherent scattering), but all have intensities which do not differ greatly from 65 % of the theoretical.

The agreement observed for the (11) and all higher-order bands shows clearly that the disparity between the (10) and (11) bands cannot be attributed to thermal agitation or to structural imperfections within the layers. Rather the high intensity of the (10) band is anomalous. This is in accordance with the observation, already made in calculating the atomic distribution function (see above), that the atomic scattering factor of James & Brindley is too low for values of s between 0·4 and 0·6. Measurements on other carbons show that the anomalously high intensity of the (10) band is of general occurrence, and a similar effect is observed for the (100) line of graphite. It is presumably due to the non-spherical character of the carbon atom in graphite-like structures. Since the (10) is the only (hk) band which occurs at values of s for which the L electrons make an appreciable contribution to the atomic scattering factor, it is here that an anomaly would be expected. A qualitative calculation shows that, if it be supposed that the electrons contained in any spherical shell at distance r from an atomic nucleus be concentrated at three points still at distance r from the nucleus but situated on the three C–C bands within a graphite-like layer, then the atomic scattering factor for the (10) band would be increased.

Assuming that 65 % of the carbon is in layers of diameter 16 A. the theoretical total intensity curve due to these layers was calculated for values of s up to 2·4. For this purpose equations (3) and (5) were used to calculate the contribution of each (hk) band at all angles up to $s = 2{\cdot}4$, the theoretical constant in the equations being multiplied by 0·65. To the sum of the intensities of the (hk) bands was added the (00) band calculated for non-parallel layers. From equation (5) this is given, for 100 % layer structure, by

$$I = K\frac{mF^2}{4\pi n A_a} s^{-2} = 0{\cdot}0606 s^{-2}, \qquad (6)$$

for all but very small angles. Since in the present case the parallelism of the layers is so slight that the (002) band is very weak and the (004) and higher orders are not detectable, the above equation, multiplied by 0·65, should represent adequately the (00) contribution for values of s greater than about 0·4.

When the total intensity curve calculated in this way is compared with the experimental curve it is found that agreement is very good if the zero of intensity in the calculated curve is placed at $I = 0{\cdot}35$ on the experimental curve (Fig. 8). Thus the calculated curve gives independent confirmation that 35 % of the carbon does not participate in the layer structure. The experimental results are satisfactorily interpreted by supposing 65 % of the carbon to be in the form of graphite-like layers of 16 A. diameter and 35 % to be in a form so disordered that the X-ray scattering due to it is indistinguishable from the independent scattering curve.

The agreement between the observed and calculated intensities for large values of s shows that the layers, although only 16 A. in diameter, are highly perfect in structure. The influence of thermal vibration within the layer is negligible.

The agreement between the observed and calculated form of the bands (particularly the (11) and (20) bands) at angles remote from the position of maximum intensity shows that the layers are perfectly planar. Slight deviation from planarity would cause the intensity of each band to decrease more rapidly with increasing angle.

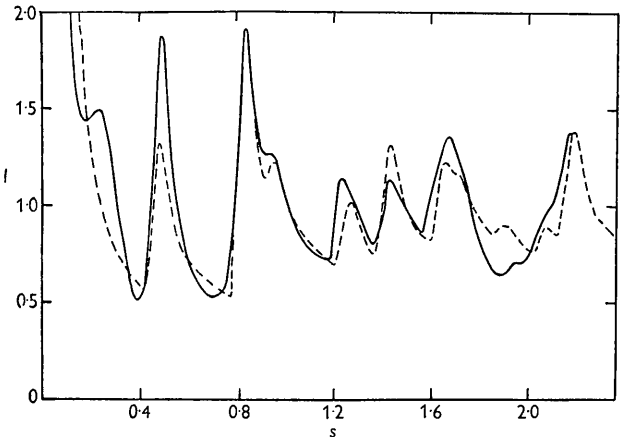

Fig. 8. The observed (corrected) intensity curve (full line) compared with that calculated (broken line) for 65 % of the carbon in the form of independent graphite-like layers of diameter 16 A., and 35 % in a highly disordered state giving a gas-like contribution to the scattering.

The (002) *band*

The (002) band, as is seen in Fig. 8, takes the form of a modulation of the (00) band given by equation (6). It is extremely diffuse, showing that it results from groups of parallel layers which each contain only a very small number of layers. Using equation (6), the intensity of the band is given by

$$I'_{002}=0{\cdot}0606s^{-2}\Sigma\frac{P_N\sin^2(\pi N d_N s)}{N\sin^2(\pi d_N s)}, \qquad (7)$$

where d_N is the inter-layer spacing in groups of N parallel layers, and P_N is the fraction of the total carbon contained in such groups. For $N=1$ this reduces to equation (6).

It is obvious that the fraction of the carbon which does not take part in the layer structure does not contribute to the (002) band. It will be assumed that the intensity in the region of the (002) band resulting from the 35 % unorganized carbon is constant and equal to 0·35, as was found to be true at larger angles. Then

$$I'_{002}=I'-0{\cdot}35, \quad \text{where} \quad I'=I/Nf^2=i(s)+1,$$

and $$\Sigma P_N=0{\cdot}65.$$

In Fig. 9, $\dfrac{(I'-0{\cdot}35)}{0{\cdot}65\times0{\cdot}0606}s^2=\dfrac{(I'-0{\cdot}35)}{0{\cdot}0394}s^2$ is plotted against s. The curve is symmetrical, and the position of the maximum gives $d=3{\cdot}70$ A. Using this value of d, the form of the band was calculated for $N=2$. Fitting the maximum and minimum of the experimental and calculated curves it was found that the agreement was very close (Fig. 8). But the amplitude of the calculated curve shown in Fig. 8 corresponds to only 70 % of the graphite-like layers. The height of the minima in the experimental curve, on the other hand, corresponds to 55 % of the layers with $N=1$, that is, to 55 % of the layers with no particular mutual orientation. The excessive total scattering must be attributed to experimental error together with the error involved in the establishment of the absolute intensity scale and the subtraction of the intensity due to the 35 % unorganized carbon. We may therefore suppose that about 55 % of the layers are grouped in parallel pairs and 45 % are isolated.

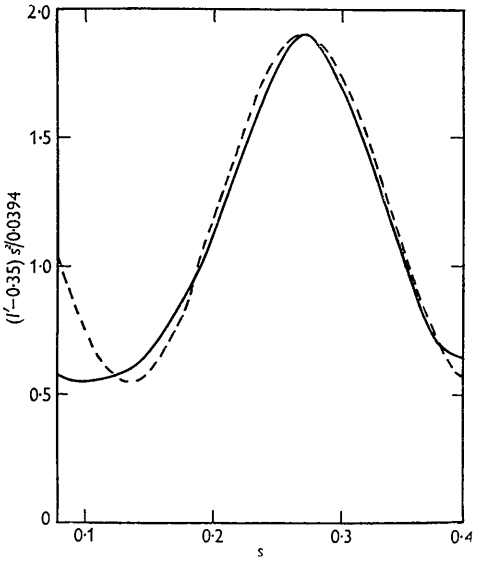

Fig. 9. The (002) band. The experimental curve (full line) is compared with that calculated (broken line) for pairs of parallel layers having separation 3·70 A.

It might be suggested that the experimental curve could be interpreted by supposing that both N and d vary, but this seems unlikely. The width of the theoretical curve for $N=3$ is only about $\frac{2}{3}$ that for $N=2$, and the variation of d required to reproduce the experimental curve with $N=3$ would therefore be very large and would involve unreasonably small values of d at one extreme. Further, if d_N varied primarily with N the experimental curve would be unsymmetrical, whereas it is not significantly so. If the mean value of d were independent of N, the variation might be expected to be greatest for small values of N, and in particular for $N=2$. Any substantial variation of d for $N=2$ would, however, result in a broadening of the base of the curve which is not observed. It seems, therefore, simplest and most reasonable to assume that the observed (002) band is due almost entirely to pairs of parallel layers, and that these account for about 55 % of all the layers present.

Low-angle scattering

For a carbon consisting entirely of large and isolated graphite-like layers or groups of parallel layers the low-

angle scattering is the (000) reflexion given by equation (7). For small layers the intensity would be slightly greater except at extremely small angles. It has been shown that in the present case only about 65 % of the carbon is in the form of graphite-like layers; a part of the intensity curve calculated according to equation (7) for 65 % of the carbon is shown in Fig. 8 for $N=1$. For $N>1$ the calculated intensity takes larger values at small angles. The experimental intensity curve takes consistently smaller values, the difference increasing rapidly with decreasing angle. It is obvious that the real structure of the carbon is remote from the ideal case of isolated layers or groups of layers, and interference between neighbouring particles must be responsible for a large reduction in the intensity of the observable low-angle scattering. The disposition of the 35 % non-organized carbon must also have some influence. If it is uniformly distributed in the spaces between the layer structure, it will serve merely to decrease the contrast in electron density of the particles and 'holes' and thus to decrease uniformly the intensity of the low-angle scattering. If it is otherwise grouped, it will affect the form of the intensity curve. A study of the relative importance of these two effects must await measurements on other carbons.

Conclusion

Comparison of the experimental and calculated intensity curves indicates that 65 % of the carbon is in the form of highly perfect and planar graphite-like layers of diameter 16 ± 1 A., and 35 % is in a highly disordered form. About 55 % of the graphite-like layers are grouped in pairs of parallel layers with an interlayer spacing of 3·7 A., and 45 % of the layers show no mutual orientation.

Interpretation of the low-angle scattering by this method would be complicated and has not been attempted.

Discussion

Methods

The agreement between the results obtained by the two methods is satisfactory. Since the Fourier-analysis method is direct and involves no assumptions or approximations, the agreement provides confirmation of the validity and usefulness of the Warren equations. The approximations involved in the derivation of these equations are seen to be admissible even for layers of diameter as small as 16 A.

Both methods involve ultimately the comparison of a curve derived from experiment with one calculated for a hypothetical structure; in one case the hypothetical structure is used to calculate the function $4\pi r^2\Delta\rho$ and in the other to calculate the intensity curve. In the present case the calculation of the high-angle part of the intensity curve is found to be particularly simple, and for future work on similar materials this method is to be preferred. Since the structural element is a single layer of perfectly coplanar identical atoms, the form of the two-dimensional bands can be calculated without complications due to a varying structure factor. And a further important simplification results from the sharp division which is observed between the organized and non-organized parts, the latter giving simply a gas-like contribution to the total scattering. Moreover, the information obtained is more precise and more extensive than that given by the Fourier analysis method, and the labour involved is less.

For the interpretation of the low-angle scattering, on the other hand, the calculation of the Fourier transform is both rapid and useful.

It may be noted that the analysis of the (002) band given above is essential for the determination of the interlayer spacing from a band so diffuse. That is, before the spacing can be measured it is necessary to obtain the intensities on the absolute scale, to subtract the Compton scattering and divide by the atomic scattering factor, and then, from a study of the (hk) bands, to determine the proportion of non-organized carbon. The scattering due to this must then be subtracted before multiplying by s^2 to obtain a symmetrical curve the position of whose maximum gives the true spacing. In the present case, before dividing by the scattering factor there is no maximum corresponding to the (002) band. After subtracting the incoherent scattering and dividing by the scattering factor the position of the maximum corresponds to a spacing of 4·2 A. The maximum obtained by multiplying by s^2 without first subtracting the contribution of the non-organized part corresponds to 3·5 A. The true spacing was found to be 3·7 A.

Structure

It is perhaps necessary to emphasize that the structure described in this paper is not to be considered as representative of all carbons. In particular the parallel stacking of the graphite-like layers appears to be exceptionally little developed. The material was selected primarily as being well suited to an investigation of available methods of analysis. Nevertheless, certain factors involved are of general interest.

It is shown that the graphite-like layers, although only 16 A. in diameter, are planar and highly perfect in structure. Thermal vibrations in the plane of the layer are negligible. The bond length is, within experimental error, the same as in graphite (1·42 A.) (Nelson & Riley, 1945). This is in agreement with the work of Bradburn, Coulson & Rushbrooke (1948). These authors calculated the bond length in rectangular graphite-like layers as a function of the number of carbon hexagons along the sides of the rectangle. They obtained 1·416 A. for the bond length in true graphite, and values greater than 1·410 A. for all layers containing more than four hexagons in each direction. A layer diameter of 16 A. corresponds roughly to six hexagons.

The interlayer spacing of 3·7 A. is very different from the graphite value, 3·35 A. This is presumably due to

the very small number of parallel layers per group, few groups containing more than two layers.

I am deeply indebted to Monsieur J. Desmaroux and Monsieur M. Mathieu for providing facilities for this work in their laboratory, and to Monsieur J. Méring for his guidance and very generous help throughout the work.

References

BISCOE, J. & WARREN, B. E. (1942). *J. Appl. Phys.* **13**, 364.

BLAYDEN, H. E., GIBSON, J. & RILEY, H. L. (1944). *Conference on the Ultra-fine Structure of Coals and Cokes.* London: British Coal Utilization Research Association.

BRADBURN, M., COULSON, C. A. & RUSHBROOKE, G. S. (1948). *Proc. Roy. Soc. Edinb.* **62**, 336.

BRAGG, W. L. & WEST, J. (1930). *Phil. Mag.* **10**, 823.

COMPTON, A. H. & ALLISON, S. K. (1935). *X-rays in Theory and Experiment.* London: Macmillan.

DEBYE, P. & MENKE, H. (1931). *Ergebn. tech. Röntgenk.* **2**, 1.

EWALD, P. P. (1940). *Proc. Phys. Soc. Lond.* **52**, 167.

FRANKLIN, R. E. (1950). *Acta Cryst.* **3**, 158.

GINGRICH, N. S. (1943). *Rev. Mod. Phys.* **15**, 90.

GUINIER, A. (1939). Thesis, University of Paris.

JAMES, R. W. (1948). *Acta Cryst.* **1**, 132.

JAMES, R. W. & BRINDLEY, G. W. (1931). *Phil. Mag.* **12**, 104.

NELSON, J. B. & RILEY, D. P. (1945). *Proc. Phys. Soc. Lond.* **57**, 477.

WARREN, B. E. (1934). *J. Chem. Phys.* **2**, 551.

WARREN, B. E. (1941). *Phys. Rev.* **9**, 693.

WILSON, A. J. C. (1948). *X-ray Optics.* London: Methuen.

Acta Cryst. (1950). **3**, 121

Structures of Molecular Addition Compounds. I. Monomethyl Amine–Boron Trifluoride, H_3CH_2N–BF_3

BY S. GELLER AND J. L. HOARD

Baker Laboratory of Chemistry, Cornell University, Ithaca, New York, U.S.A.

(*Received* 20 *April* 1949 *and in revised form* 25 *July* 1949)

X-ray data obtained from crystals of H_3CH_2N–BF_3 lead to a monoclinic unit of structure with $a=5{\cdot}06$, $b=7{\cdot}28$, $c=5{\cdot}81$ A., $\beta=101°\ 31'$, containing two stoichiometric molecules. All of the X-ray data are consistent with the space group $P2_1/m$. Approximate positions of the atoms (other than hydrogen) were determined by the use of various Patterson syntheses, and the parameters refined by means of various Fourier syntheses.

There are several important and interesting features of the structure of H_3CH_2N–BF_3. The B–N bond is 1·58 A., 0·09 A. longer than the value predicted on the basis of Pauling's covalent radii with application of a correction for difference of electronegativity between boron and nitrogen. Yet the compound is stable at ordinary temperatures. The nitrogen atom does not form four equivalent tetrahedral bonds in H_3CH_2N–BF_3 ($\angle$B–N–C = 114°). The methyl group and fluorine atoms are in the staggered configuration.

The deviations of the F–B–F angle (111°) and the F–B–N angle (108°) from the tetrahedral value (109° 28′), of the value for the B–F bond (1·37 A.) from the predicted value, 1·39 A. (Schomaker & Stevenson, 1941; Bauer & Beach, 1941), and of the C–N bond (1·50 A.) from 1·47 A. cannot be said to be very significant since the limits of error may be such as to make these differences unreal. On the other hand, there is some evidence from the results of the X-ray diffraction investigation of H_3CCN–BF_3 (the second paper in this series) and of the electron diffraction investigation of $(H_3C)_2O$–BF_3 that indicates that these differences are possible. The results of the former study leave little doubt that the boron atom need not form four equivalent tetrahedral bonds, whereas the results of the latter give some indication that the stretching of the C–N bond in H_3CH_2N–BF_3 is probable.

All of the important interatomic distances have been calculated and the packing arrangement of the molecules in the crystal is discussed.

Introduction

The discovery, in recent years, of many new boron compounds, and of interesting and important properties of both old and new compounds, has led to increased study of them.

It is generally considered that in molecules such as the boron trihalides or trimethyl boron, boron has a strong tendency to complete its octet of valency electrons by forming a fourth bond. It is also postulated that the nitrogen atom in NH_3 and in substituted ammonias possesses a pair of unshared electrons which tend to form a fourth bond. In this investigation, the particular interest is in the compound formed by the reaction in equimolar ratio of BF_3 and H_3CNH_2. In this